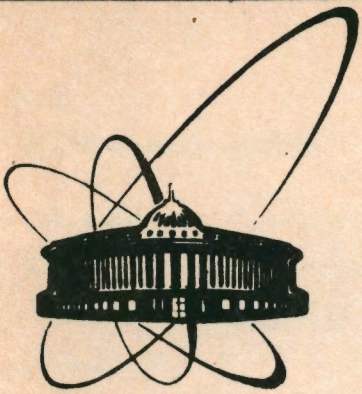

объединенный
институт
ядерных
исследований
дубна

E2-92-103

S.V. Goloskokov

QUARK-LOOP EFFECTS IN HIGH ENERGY SPIN-FLIP PROCESSES

Submitted to "Journal of Physics G: Nuclear and Particle Physics"

1992

1 Introduction

The problem of existence of large spin effects in different reactions [1] is very important now. The standard perturbative QCD cannot explain such experimentally observable phenomena because it leads to a power suppression of the spin-flip amplitude at large momenta transfer [2].

Here we shall be interested in the hadron reactions at high energies and fixed momenta transfer, where the exchange with vacuum quantum numbers in the t-channel (pomeron) play an important role. Really, it gives a leading contribution to the elastic hadron scattering amplitude. The pomeron exchange must be taken into account for inelastic exclusive processes as a rescattering. So the pomeron spin structure can lead to the essential spin effects which are observed in the binary reactions in this kinematic region where the perturbative theory cannot be used.

The vacuum t-channel amplitude is usually associated in QCD with the two-gluon exchange [3]. The spinless pomeron was analysed in [4, 5, 6] on the basis of a QCD model with taking account of the nonperturbative properties of the theory. A similar model was used for investigation of the spin effects in pomeron exchange . It was shown that different contributions like a gluon ladder [7] and quark loops [8, 9] may lead to the spin-flip amplitude growing as s in the $s \to \infty$ limit. There was obtained the following ratio

$$\frac{\mid T_{flip} \mid}{\mid T_{non-flip} \mid} \simeq \frac{m\sqrt{\mid t \mid}}{a(m,t)\ln s/s_0}. \qquad (1)$$

Here and in what follows $m = .33GeV$ is the constituent quark mass and a is a function linearly dependent on $\mid t \mid$ at large $\mid t \mid$.

This result is due to the absence of the spin effects only in the leading log approximation in the whole amplitude. In all cases the spin effects nonvanishing in the

high energy limit are determined by the low-energy subgraph accompanied by the high energy two-gluon exchange. As a result, such spin effects are connected with the nonperturbative long-distances contributions.

However, the quantitative calculations in QCD in the nonperturbative region is impossible now. Different model approaches are used for describing the high energy hadron interaction at fixed momenta transfer. Some of them lead to the spin effects which do not disappear in high energy processes, including elastic scattering [10, 11]. In the paper [11] the dynamical model was proposed in which the contribution of the nucleon meson-cloud to the spin effects was investigated. This model explains spin phenomena in different hadron reactions quantitatively [12].

It is very important to investigate the quark-sea effects on the spin-flip processes at high energies in the QCD long-distance model because they are very similar to the meson-cloud model from the phenomenological point of view. In the second part of the paper we shall calculate such effects for the qq scattering at high energies and fixed momenta transfer.

It is known that the large distances contributions from the hadron wave function (see [13, 14] e.g.) can lead to the spin effects which do not vanish at high energies. To estimate the relative role of spin effects from the wave function and the elementary quark subprocess, we calculate in the third part the $\gamma q \to \gamma q$ scattering as an example. Some details of integral calculations can be found in the Appendix A.

2 Quark-sea contribution to qq subprocess at high energies

Let us investigate the quark-quark scattering

$$q(p_1) + q(p_2) \to q(p_3) + q(p_4)$$

that plays an important role in different high energy processes at fixed momentum transfer.

In what follows we shall use the symmetric coordinate system in which the sum

of quark momenta before and after scattering is directed along the z-axis [7]

$$p = \frac{p_1 + p_3}{2},\ p' = \frac{p_2 + p_4}{2},\ p^2 = p'^2 = m^2 - \frac{t}{4},\ t = (p_1 - p_3)^2,\ s \simeq 2(pp'). \quad (2)$$

The α_s^3 contribution to the qq spin-flip scattering amplitude in the $s \to \infty$, t-fixed limit was calculated in [7]. In [8, 9] the role was investigated of the quark loops in the t-channel two-gluon exchange.

However there are other diagrams with the quark loops determined by the quark sea. It will be shown that these contributions can be very important in soft processes. One of these diagrams can be seen in Fig.1a. There are some gluon exchanges between quark-antiquark pairs in the t-channel. The confinement effects combine them together. These nonperturbative objects can be approximated, using the effective-meson-lagrangian method, [15] by two meson states. In the case of $qq\pi$ coupling this lagrangian has the form (the isospin factor is not included):

$$L_{\pi qq} = i g_\pi \bar{q}^\alpha \gamma_5 q^\alpha \pi$$

with $\alpha_\pi = g_\pi^2/4\pi \simeq 1$. As a result, we have effective diagrams of Fig.1b,c. These diagrams are accompanied by similar graphs with the crossed gluon lines. It can be shown that the real parts of amplitudes compensate each other for the color-singlet state in the t-channel. Thus the leading term of the scattering amplitude is approximately purely imaginary for the pomeron exchange. In these calculations we must use the perturbative s-channel quark propagators [17].

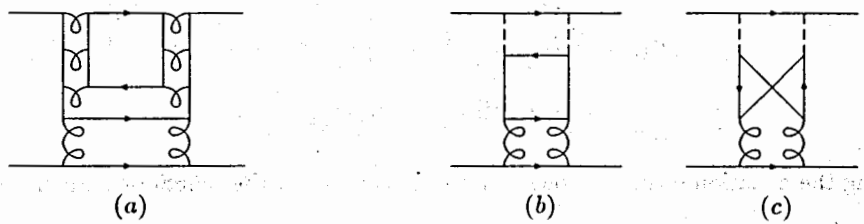

Fig. 1 (a)-An example of the quark-sea contribution to the scattering amplitude. (b),(c)-Effective meson diagrams with the quark-loop.

So let us investigate only the imaginary part of the graphs, Fig.1b,c. The calculations are performed in the light-cone variables as in papers [7, 8]. After integration with

the δ-function we obtain the following representation for the amplitude Fig.1b

$$\mathrm{Im}T^b(s,t) = 2c^b \frac{\alpha_s^2 \alpha_\pi^2}{(2\pi)^4 s} \int \frac{dxdz\theta(1-x)\theta(x-z)\theta(z-y)}{(1-x)(x-z)(z-y)}$$
$$\cdot \int d^2k_\perp d^2q_\perp d^2l_\perp \left[(\Gamma)^{up} \Pi(F\,S\,M)\, 4T_{\mu,\nu}p'^\mu p'^\nu \right] |_{k_-,l_-,q_-,y}, \qquad (3)$$

where c^b is a color factor, k_-, l_-, q_-, y are pole solutions of the δ-functions; they are written in [8].

In the form (3) $4T_{\mu,\nu}p'^\mu p'^\nu$ is a trace over the quark loop multiplied by the spin-non-flip matrix element in the down-quark line, $\Pi(F\,S\,M)$ is a product of the meson propagators, the gluon and quark functions which are determined in what follows, $(\Gamma)^{up}$ is a matrix element in the up-quark line of the form

$$(\Gamma)^{up} = \langle [m\Gamma_0 - (1-x)\Gamma_- - \frac{m^2+k_\perp^2}{(1-x)}\Gamma_+] \rangle^{up}. \qquad (4)$$

In the light-cone variables the matrices Γ in (4) are determined as follows

$$\Gamma_0 = I,\ \Gamma_1 = \frac{\sqrt{s}\gamma_-}{2},\ \Gamma_2 = \frac{\gamma_+}{2\sqrt{s}}. \qquad (5)$$

In the calculation we use the standard form of the meson propagator. The gluon and the t-channel quark propagators are in the nonperturbative region. Let us discuss the form of the quark propagator given by the representation

$$\langle 0|T\left(q^\alpha(x)\,\bar{q}^\beta(y)\right)|0\rangle = \frac{\delta^{\alpha\beta}}{i}\hat{S}(x-y).$$

For the perturbative part of $\hat{S}(x-y)$ the standard representation is fulfilled and for the nonperturbative part we use the following form

$$\hat{S}^{np}(x-y) = \frac{1}{(2\pi)^4}\int d^4p\,\hat{S}(p)\,e^{-ip(x-y)} =$$
$$\frac{1}{(2\pi)^4}\int d^4p\,(m\tilde{B}(p^2) + \hat{p}\tilde{A}(p^2))\,e^{-ip(x-y)}. \qquad (6)$$

Using the equation of motion one can relate integrals of the functions $\tilde{A}, \tilde{B}$ from (6) with the quark condensate

$$\frac{m}{i(2\pi)^4}\int d^4p\,\tilde{B}(p^2) = -\frac{\langle\bar{q}q\rangle}{12}, \qquad (7)$$
$$\frac{1}{i(2\pi)^4}\int d^4p\,p^2\tilde{A}(p^2) = -\frac{m\langle\bar{q}q\rangle}{12} + O(g).$$

Similar equations were obtained in [16, 17]. It is easy to see that the second equation in (7) cannot be used in the nonperturbative region because of large g corrections. So we shall use the first one.

Let us perform our calculations for two forms of the nonperturbative quark propagator. The first is the "scalar" form [18]

$$\hat{S}_s^{np}(p) = \frac{h_s^q}{m_1}\,e^{p^2/m_1^2} = \frac{h_s^q}{m_1}\,S(p^2). \qquad (8)$$

The second is a form equivalent to the perturbative one used in [17]

$$\hat{S}_p^{np}(p) = \frac{h_p^q}{m_1^2}(\hat{p}+m_1)\,e^{p^2/m_1^2} = \frac{h_p^q}{m_1^2}(\hat{p}+m_1)\,S(p^2). \qquad (9)$$

The propagators (8,9) decrease exponentially in the investigated region. The magnitudes of h_q^s and h_q^p can be obtained from (7)

$$h_s^q = h_p^q = h_q = \frac{4\pi^2}{3}(\frac{m_0}{m_1})^3, \qquad (10)$$

where $m_0 \approx .225GeV$ determines a quark condensate value $\langle\bar{q}q\rangle = -m_0^3$.

The value of m_1 in (8) is connected directly with the magnitude of λ in the exponential parametrization of a nonlocal quark condensate $m_1^2 = \lambda^2/2$. Using [18, 19] we find that m_1 can change in the interval

$$m_1 = (0.4 \div 0.5)GeV. \qquad (11)$$

For the propagator in the form (9) in [17] there was used the value $m_1 = .33GeV$. We shall change it in the interval

$$m_1 = (0.33 \div 0.4)GeV. \qquad (12)$$

In the nonperturbative gluon propagator

$$G_{\alpha\beta}^g(q) = -ig_{\alpha\beta}F^{np}(q^2) \qquad (13)$$

we use the simplest exponential form for the $F^{np}(q^2)$ function [6, 17]

$$F^{np}(q^2) = h_g\,e^{bq^2}. \qquad (14)$$

Discussion of the magnitudes of h^g and b can be found in [4, 17]. Their values are unimportant here.

It is easy to see that the integrals over $d^2l_\perp$ and $d^2q_\perp$ in (3) have an exponential form and the integrations over these variables are trivial. Integration over $d^2k_\perp$ can be performed easily with the help of α representation. But in this case we shall obtain an additional integral. However in the soft region where we use an exponential form for nonperturbative t-channel propagators it is not necessary to calculate integrals explicitly. We use the approximations (A3,A4,A5) and (A6,A7) in calculations of the integrals for simplicity (see Appendix A for details). The remained two-dimensional integral was calculated numerically.

Let us discuss the matrix structure of the obtained scattering amplitude. The form (5) can be rewritten in terms of the "Sudakov" momenta

$$\hat{\Gamma}_0 = I,\ \hat{\Gamma}_1 = \hat{\tilde{p}},\ \hat{\Gamma}_2 = \frac{\hat{\tilde{p}'}}{s}, \tag{15}$$

where

$$\tilde{p} = p - \frac{p^2}{s}p',\ \tilde{p'} = p' - \frac{p^2}{s}p,\ \tilde{p}^2 = \tilde{p'}^2 = 0.$$

As a result , we get the following structure of the amplitude (3)

$$T^b(s,t) \simeq isc^b\,[\frac{\pi}{2b}\alpha_s^2\,h_g^2\,e^{bt/2}]\,B\,[\,t_0\frac{\Gamma_0}{m} + t_1\frac{\Gamma_1}{m^2} + t_2\,\Gamma_2\,] \otimes \frac{\hat{\tilde{p}}}{s}. \tag{16}$$

Here the constituent quark masses are introduced in order to obtain the same dimensions of t_i amplitudes. The $\hat{\tilde{p}}/s$ term is present in (16) because in the down-quark line the helicity is conserved as in the case of the simplest two-gluon exchange (see [4] e.g.)

$$\langle\frac{\hat{\tilde{p}}}{s}\rangle_{++}^{down} = 1,\ \langle\frac{\hat{\tilde{p}}}{s}\rangle_{+-}^{down} \sim 0.$$

In (16) B has the form

$$B = (\frac{\alpha_\pi\,h_q}{\pi})^2. \tag{17}$$

It is easy to see that the simplest two-gluon exchange graph that contributes to the leading asymptotic term of the scattering amplitude looks as follows

$$T^{2g}(s,t) = A^{2g}(s,t)\,[\frac{\hat{\tilde{p}'}\otimes\hat{\tilde{p}}}{s^2}], \tag{18}$$

where

$$A^{2g}(s,t) = 4isc^{2g}[\frac{\pi}{2b}\alpha_s^2\,h_g^2\,e^{bt/2}] \tag{19}$$

is the spin-non-flip amplitude of the two-gluon exchange [4]. Note that we have a similar term in (16) as a coefficient.

Combining this contribution with the calculated amplitude, Fig.1b, and the corresponding reversed graph we obtain

$$T(s,t) = A^{2g}(s,t)\,\{\hat{M}_2 + [\,T_0\,\hat{M}_0 + T_1\,\hat{M}_1 + 2\,T_2\,\hat{M}_2\,]\}, \tag{20}$$

where we use the following definitions of the matrix structure

$$\hat{M}_0 = \frac{I\otimes\hat{\tilde{p}} + \hat{\tilde{p}'}\otimes I}{sm},\ \hat{M}_1 = \frac{\hat{\tilde{p}}\otimes\hat{\tilde{p}} + \hat{\tilde{p}'}\otimes\hat{\tilde{p}'}}{sm^2},\ \hat{M}_2 = \frac{\hat{\tilde{p}'}\otimes\hat{\tilde{p}}}{s^2}. \tag{21}$$

The T_i in (20) are related with t_i from (16) by the condition $T_i = 3/4\,B\,t_i$. Using (10) we have

$$T_i = \frac{4\pi^2\alpha_\pi^2}{3}[\frac{m_0}{m_1}]^6\,t_i. \tag{22}$$

The amplitudes T_i calculated for two different forms of the quark propagator (8,9) are shown in Fig 2(a-c). It is easy to see that for the same value of the mass $m_1 = .4GeV$ we obtain very similar results in both the cases.

The nonplanar contribution (Fig 1c) was investigated too. In this case we have a region where both the quark propagators are nonperturbative as before. The calculation for the diagram in Fig 1c is more complicated and we do not want to discuss its details. We have a form similar to (20) as a result. But the obtained amplitudes are suppressed by a factor about 10 with respect to the planar contribution (see Fig 2b as an example). The same suppression is true for particles heavier than the π-meson.

So we can conclude that the main contribution to the scattering amplitude at high energies and small t comes from the planar diagram with the π-mesons exchange in the t-channel. The quark-sea effects drastically change the matrix structure of the simplest 2-gluon exchange which has only the $\hat{M}_2$ term (18,20). The new $\hat{M}_0$ and $\hat{M}_1$ terms result in the spin-flip amplitude growing as s.

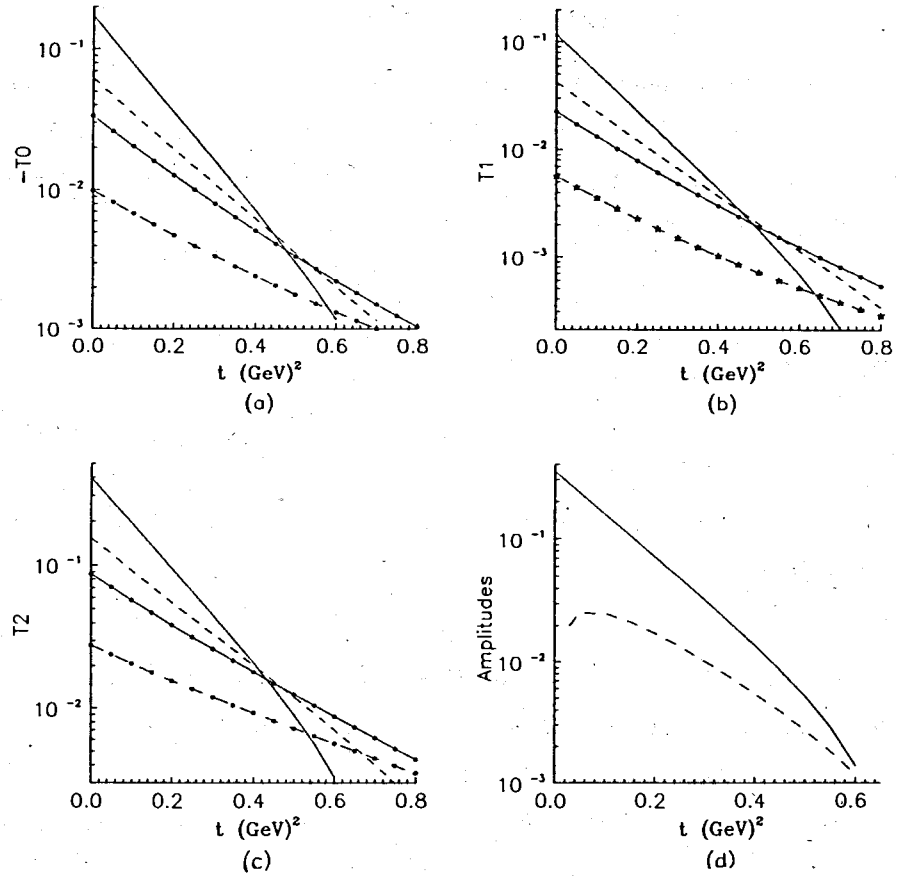

Fig.2(a)-(c)-Amplitudes $T_0 - T_2$ from (20) for different choices of quark propagators: For the case (9): solid line-for $m_1 = .33GeV$; dashed line-for $m_1 = .4GeV$. For the case (8): solid line with dots-for $m_1 = .4GeV$; dashed line with dots-for $m_1 = .5GeV$.

In **Fig.2b** the dashed line with stars-is a contribution of the nonplanar graph for the case (9) with $m_1 = .33GeV$.

Fig.2d-solid line - T^{nf}_{sea} determined in (23), dashed line -T^{f}_{sea} from (24) for the case (9) with $m_1 = .33GeV$.

Calculating the corresponding matrix elements from (20) we obtain

$$T^{nf}(s,t) = A^{2g}(s,t)\{1 + T^{nf}_{sea}\},$$
$$T^{nf}_{sea} = 2[2T_0 + T_1(1 + \frac{t}{4m^2}) + T_2]; \quad (23)$$
$$T^{f}(s,t) = A^{2g}(s,t)\,T^{f}_{sea},$$
$$T^{f}_{sea} = \frac{\sqrt{|t|}}{m}\{T_0 + T_1\}. \quad (24)$$

The resulting T^{nf}_{sea} and T^{f}_{sea} are shown in Fig.2d where one can see the model results for the quark propagators in the form (9). Note that the magnitude of T^{nf}_{sea} is not very small as compared to 1. It should renormalise the magnitude of h_g determined for the simplest 2-gluon exchange (see [17] e.g.). However the magnitude of T^{f}_{sea} is sufficiently small. Really it is about 10% of T^{nf}_{sea} and only about 1% of the nonflip amplitude of the two-gluon exchange. This smallness is a result of the compensation between T_0 and T_1 in (24) because they are approximately of the same magnitude and opposite in sign (Fig.2a,b).

3 Spin effects in $\gamma q \to \gamma q$ scattering

Large distance contributions from the hadron wave function can lead to additional spin effects which do not vanish at high energies [13, 14]. Moreover the new matrix structure of the high-energy quark-quark subprocess obtained in the previous part of the paper can change the spin structure in the hadron amplitude determined by the long-distance effects from the hadron wave functions as compared to the simple spinless pomeron exchange. So it is important to determine the relative role of spin effects from the wave function and the elementary quark subprocess.

Of course there are diagrams in which the pomeron couples with two different quarks in a hadron. But these contributions can be suppressed because of the integration with the hadron wave functions (see [4] e.g.). As a result the pomeron must prefer to interact with a single quark in the hadron. We shall investigate such graphs in what follows. It is easy to see that the contributions from the hadron wave

function are very similar to the loop-integral in high energy γq scattering (see Fig.3). This process is not a hadron reaction. However all calculations can be performed up to the end in the case of quark-photon scattering without taking into account any additional information about the hadron spin structure.

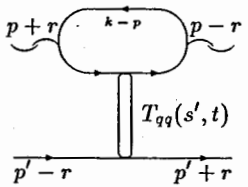

Fig.3 The high-energy contribution to the γq scattering amplitude.

So let us examine this reaction at high energies and fixed momenta transfer as tool for estimation of the contributions from different interaction regions to the helicity amplitudes. As previously, we shall calculate only the imaginary part of the leading term of the scattering amplitude. In calculations we shall use the form (9) for nonperturbative quark propagators. As a result,

$$\mathrm{Im}T^{\gamma q}_{\lambda_2\lambda_1}(s,t) = 3\sum_{f=1}^{n_f}\frac{Q_f^2}{16\pi^3}(\frac{h_p^q}{m_1^2})^2\int d^4k\delta((p-k)^2-m_1^2)S(k+r)S(k-r)$$
$$\epsilon_\nu^{\lambda_2*}(p-r)T^{\nu\mu}\epsilon_\mu^{\lambda_1}(p+r). \qquad (25)$$

Here $S(p)$ is a function given in the quark propagator (9), $\epsilon_\mu^{\lambda_1}(p+r)$ and $\epsilon_\nu^{\lambda_2}(p-r)$ are initial and final polarization vectors. We shall suppose that initial polarization is positive and final is arbitrary. In this case for the coordinate system determined in (2) the polarization vectors are of the form

$$\epsilon_\mu^{+1}(p+r) = (0,-\cos(\theta/2),-i,-\sin(\theta/2)),$$
$$\epsilon_\nu^{\lambda}(p-r) = (0,-\lambda\cos(\theta/2),-i,\lambda\sin(\theta/2)), \qquad (26)$$

where θ is a scattering angle.

In (25) $T^{\nu\mu}$ is a trace over a quark loop which includes the matrix structure of quark-quark scattering amplitude $\langle T(s',t)\rangle_{down}$ from (20). For this amplitude we calculate the spin-non-flip matrix element in the down quark line. To separate spin effects from the quark-loop and the meson-cloud, we shall calculate the simple two

gluon exchange and the sea contributions independently. For the two-gluon amplitude (18) we have

$$\langle T^{2g}(s,t)\rangle_{down} = A^{2g}(s,t)[\frac{\hat{p'}}{s}]. \qquad (27)$$

For the sea contribution one can obtain from (20)

$$\langle T^{sea}(s,t)\rangle_{down} = A^{2g}(s',t)\{\frac{\hat{p'}}{s'}[2T_0 + T_1\frac{p'^2-k^2}{m_1^2} + 2T_2] + T_0\frac{I}{m_1} + T_1\frac{\hat{k}}{m_1^2}\}. \qquad (28)$$

The functions T_i are determined in (22). These expressions are used for calculations of the gluon spin-flip and spin-non-flip amplitude on quark which do not change its helicity. We do not want to discuss here the details of calculations. The obtained result can be represented in the form

$$T^{\gamma q}_{\lambda_2+}(s,t) = i(4\pi\alpha)A^{2g}(s,t)\Phi^{\gamma q}_{\lambda_2+}(t). \qquad (29)$$

Here $\alpha = 1/137$.

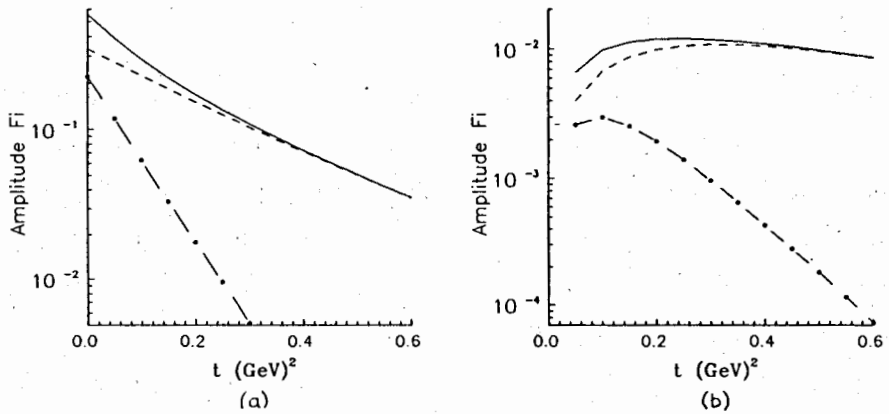

Fig.4 (a)- $\Phi^{\gamma q}_{++}(t)$ amplitude determined in (29): dashed line-the simple two-gluon contribution; dashed line with dots-the quark-sea contribution; solid line-the total result. (b)- the same for $\Phi^{\gamma q}_{-+}(t)$ amplitude.

The simple two-gluon exchange contribution, the sea effects, the total functions $\Phi^{\gamma q}_{++}(t)$ and $\Phi^{\gamma q}_{-+}(t)$ are shown in Fig.4. We can see from Fig.4a that the sea contribution is very important at small momenta transfer. This long-distance effect gives

about 40% of the total spin-non-flip amplitude at $t = 0$ and decreases quickly with $|t|$ growing, which is caused by the large slope in the quark t -channel propagators (9,12). As a result, the behavior of $\Phi^{\gamma q}_{++}(t)$ at $|t| \geq 0.3\ Gev^2$ is determined only by the two-gluon exchange. The obtained spin-flip amplitude is sufficiently small (see Fig.4b) but this is connected with the choosen process. The most important is the fact that with taking account of the kinematical factor $|t|$ in the spin-flip amplitude, the sea contribution to $\Phi^{\gamma q}_{-+}(t)$ is of the same order of magnitude as the corresponding effect in $\Phi^{\gamma q}_{++}(t)$. Really it is about 30% of the total spin-flip amplitude at $|t| \simeq 0.1\ Gev^2$. This large magnitude of the sea effects is due to the fact that different contributions are not compensated in the loop integral as in the case of a simple matrix element (see (24)). The behavior of $\Phi^{\gamma q}_{-+}(t)$ is determined by the two-gluon contribution at a larger momentum transfer as previously.

4 Conclusion

So, the $\bar{q}q$ -sea contribution in the high energy scattering as $s \to \infty$, t-fixed, makes the spin-flip amplitude growing as s. The obtained results show that the main contribution in this case is determined by the planar diagrams of the form Fig.1b. Note that the amplitude of the simple two-gluon exchange (which can be considered as a "bare" pomeron) is factorised from the large-distance effects in all the cases investigated here. In the general case it can be replaced either by a ladder gluon amplitude equivalent to the "natural" pomeron or by the quark-antiquark exchange. In all cases the matrix structure in the upper-quark line does not change. As a result, we obtain the same energy dependence of the spin-flip and spin-non-flip amplitude, as previously.

It is shown that the quark-sea effects in the scattering amplitude can reach 30-40% of the "bare" pomeron contribution. This confirms the important role of such effects in high-energy reactions. All this can explain the success of the meson-cloud model [11, 12] that takes into account similar contributions phenomenogically. Of course, we

must include the $\bar{q}q$ pairs directly from the wave functions but this problem requires an additional analysis.

So, the long-distance effects investigated here can lead to the spin flip in hadron reactions at fixed momenta transfer in the $s \to \infty$ limit and the leading asymptotic term of the scattering amplitude has a complicated spin structure. Thus, the quark loops from the sea can be an important generation mechanism of the spin effects at high energies in QCD at large distances.

Acknowledgement. The author expresses his deep grattitude to V.G.Kadyshevsky for support and to A.V.Efremov and D.Robaschik for discussion.

5 Appendix A

We rewrite the integral over $d^2k_\perp$ in the form

$$\Phi(r^2) = \int \frac{d^2k_\perp e^{-fk_\perp^2 - 2h(\vec{k}_\perp \vec{r}_\perp)}}{[\beta + (\vec{k}_\perp + (1-x)\vec{r}_\perp)^2][\beta + (\vec{k}_\perp - (1-x)\vec{r}_\perp)^2]} = \tag{A1}$$

$$\frac{1}{2}\int_{-1}^{1} d\gamma \int \frac{d^2k_\perp e^{-fk_\perp^2 - 2h(\vec{k}_\perp \vec{r}_\perp)}}{[\beta + k_\perp^2 + (1-x)^2 r_\perp^2 + 2\gamma(1-x)(\vec{k}_\perp \vec{r}_\perp)]^2}.$$

Using the α representation and integrating over $d^2k_\perp$ we have

$$\Phi(r^2) = \frac{\pi}{2}\int_{-1}^{1} d\gamma \int_0^\infty \frac{\alpha d\alpha}{f+\alpha} exp\{-\alpha\beta - r_\perp^2[\alpha(1-x)^2 - \frac{(h+\alpha\gamma(1-x))^2}{f+\alpha}]\}. \tag{A2}$$

Parametrising (A2) in the exponential form

$$\Phi(r^2) = \pi\phi e^{-r_\perp^2 \psi/\phi}. \tag{A3}$$

Comparing the magnitudes and the first derivatives with respect to $r_\perp^2$ of the functions (A1,A2) at $r_\perp^2 = 0$ we shall obtain the integral representations for ϕ and ψ. For example,

$$\phi = \int_0^\infty \frac{\alpha d\alpha}{f+\alpha} e^{-\alpha\beta} \simeq \int_0^{\frac{1}{\beta}} \frac{\alpha d\alpha}{f+\alpha} = \frac{1 - \beta f \ln((1+\beta f)/\beta f)}{\beta} \tag{A4}$$

Similar calculations give us the following form for the ψ

$$\psi = -\frac{3\beta^2 h^2(1+\beta f)\ln((1+\beta f)/\beta f) - 3\beta^2 h^2 - (1-x)^2}{3\beta^2(1+\beta f)} \tag{A5}$$

For the integral with $k_\perp^2$ in the numerator we use the similar approximation

$$\Phi_1(r^2) = \int \frac{k_\perp^2 d^2k_\perp e^{-fk_\perp^2 - 2h(\vec{k}_\perp \vec{r}_\perp)}}{[\beta + (\vec{k}_\perp + (1-x)\vec{r}_\perp)^2][\beta + (\vec{k}_\perp - (1-x)\vec{r}_\perp)^2]} = \pi\phi_1 e^{-r_\perp^2 \psi_1/\phi_1}, \quad \text{(A6)}$$

where

$$\phi_1 = \frac{(1+\beta f)\ln((1+\beta f)/\beta f) - 1}{1+\beta f}, \quad \psi_1 = \frac{(1-x)^2 f - 3\beta h^2}{3\beta f(1+\beta f)^2}. \quad \text{(A7)}$$

The obtained approximations (A3,A4,A5) and (A6,A7) reproduce the initial integrals with an accuracy better than 20% for $|t| \leq 0.8\ Gev^2$.

References

[1] S.B.Nurushev, In Proc. of the 2 Int. Workshop on High Energy Spin Phys., Protvino 1984, p.5;
A.D.Krish, In Proc. of the 6 Int. Symp. on High Energy Spin Phys., Marseille,1984, p.C2-511;
N.E.Tyurin, In Proc. of the 8 Int. Symp. on High Energy Spin Phys., Bonn, 1990, p.65.

[2] S.J.Brodsky, G.P.Lepage, Phys.Rev., 1980, v.D22, p.2157.

[3] F.E.Low, Phys.Rev., 1975, v.D12, p.163;
S.Nussinov, Phys.Rev.Lett., 1975, v.34, p.1286.

[4] P.V.Landshoff, O.Nachtmann, Z.Phys.C-Particles and Field 1987, v.35, p.405.

[5] A.Donnachie, P.V.Landshoff, Nucl.Phys., 1989, v.B311, p.509.

[6] D.A.Ross, J.Phys. G:Nucl.Part.Phys., 1989, v.15, p.1175.

[7] S.V.Goloskokov, Yad.Fis., 1989, v.49, p.1427.

[8] S.V.Goloskokov, Yad.Fis., 1990, v.52, p.246;
S.V.Goloskokov, In Proc. of the 8 Int. Symp. on High Energy Spin Phys., Bonn, 1990, p.472.

[9] S.V.Goloskokov, Yad.Fis., 1991, v.53, p.1650;
S.V.Goloskokov, Z.Phys.C-Particles and Fields 1991, v.52, p.329.

[10] J.Pumplin, G.L.Kane, Phys.Rev., 1975, v.D11, p.1183;
L.D.Soloviev, A.V.Shchelkachev, Particles and Nuclei 1975, v.6, p.571;
S.M.Troshin, N.E.Tyurin, Pis'ma ZhETF, 1976, v.23, p.716;
C.Bourrely, J.Soffer , T.T.Wu, Phys.Rev., 1979, v.D19, p.3249.

[11] S.V.Goloskokov, S.P.Kuleshov, O.V.Seljugin, Particles and Nuclei 1987, v.18, p.39.
S.V.Goloskokov, S.P.Kuleshov, O.V.Seljugin, Yad.Fis., 1989, v.50, p.779.

[12] S.V.Goloskokov, S.P.Kuleshov, O.V.Seljugin, Z.Phys.C-Particles and Fields 1991, v.50, p.455.

[13] V.L.Chernyak, I.R.Zhitnitski, Nucl.Phys., 1983, v.B222, p.382.

[14] M.Anselmino, P.Kroll, B.Pire, Z.Phys.C-Particles and Fields 1987, v.36, p.89.

[15] M.K.Volkov, Particles and Nuclei 1986, v.17, p.433.

[16] M.J.Lavelle, M.Schaden, Phys.Lett., 1988, v.208B, p.297.

[17] J.R.Gudell, A.Donnachie, P.V.Landshoff, Nucl.Phys., 1989, v.B322, p.55.

[18] S.V.Mikhailov, A.V.Radyushkin, ZhETF Lett., 1986, v.43, p.712;
Yad.Fiz. 1989 v.49 794.

[19] V.M.Belyaev, B.L.Ioffe, ZhETF 1982, v.93, p.876;
A.A.Ovchinnikov, A.A.Pivovarov, Yad.Fiz., 1988, v.48, p.1135.

Received by Publishing Department
on March 10, 1992.